



Arc erosion behaviors of AgSnO₂ contact materials prepared with different SnO₂ particle sizes

Miao ZHANG, Xian-hui WANG, Xiao-hong YANG, Jun-tao ZOU, Shu-hua LIANG

Shaanxi Key Laboratory of Electrical Materials and Infiltration Technology,
Xi'an University of Technology, Xi'an 710048, China

Received 30 April 2015; accepted 12 October 2015

Abstract: To clarify the effect of SnO₂ particle size on the arc erosion behavior of AgSnO₂ contact material, Ag–4%SnO₂ (mass fraction) contact materials with different sizes of SnO₂ particles were fabricated by powder metallurgy. The microstructure of Ag–4%SnO₂ contact materials was characterized, and the relative density, hardness and electrical conductivity were measured. The arc erosion of Ag–4%SnO₂ contact materials was tested, the arc duration and mass loss before and after arc erosion were determined, the surface morphologies and compositions of Ag–4%SnO₂ contact materials after arc erosion were characterized, and the arc erosion mechanism of AgSnO₂ contact materials was discussed. The results show that fine SnO₂ particle is beneficial for the improvement of the relative density and hardness, but decreases the electrical conductivity. With the decrease of SnO₂ particle size, Ag–4%SnO₂ contact material presents shorter arc duration, less mass loss, larger erosion area and shallower arc erosion pits.

Key words: AgSnO₂ contact materials; SnO₂ particle size; arc erosion; electrical conductivity; hardness

1 Introduction

The electrical contact materials are widely used in switches, relays, contactors and circuit breakers and their properties directly affect the stability and reliability of electric system [1–3]. Hence, it is required that the contact materials should have excellent electrical and thermal conductivities, erosion resistance, welding resistance and low contact resistance [4–6]. Though AgSnO₂ contact material has shown a promising prospect due to its environmental benign and remarkable performances [7–12], the arc erosion mechanism of AgSnO₂ contact material is still obscure so far. RIEDER and WEICHSLEDER [13] thought that the arc erosion is strongly influenced by the mechanical action. RONG [14] found out that the arc erosion depends on the surface dynamics of AgSnO₂ material. BEHRENS et al [15] reported that the arc erosion resistance is correlated with the microstructure and mechanical strength of AgSnO₂ material after arc erosion. DU et al [16] believed that the arc erosion depends on the thermodynamic properties of each component, the

surface composition and microstructure, as well as the dynamic response of the molten pool to the arc. ZHU et al [17,18] revealed that the wettability of Ag and SnO₂ plays an important role in the arc erosion behavior. LUNGU et al [19] and WANG et al [20] thought that the structure homogenization obviously affects the arc erosion resistance of AgSnO₂ material. WITTER and CHEN [21] found out that the SnO₂ content is of major importance for erosion resistance. SWINGLER and SUMPTION [22] reported that the erosion mechanism is related to the element species of the contact materials during the arc discharge. XU et al [23] found out that the input energy of the arc is crucial to the arc erosion of AgMeO contact materials in comparison with the MeO density, thermal conductivity and volume fraction of MeO. ZHANG et al [24] believed that the erosion behavior is the combined action of materials, circuit parameters and the service environment. LIN et al [25] reported the effect of SnO₂ particle size on the microstructure and physical properties of AgSnO₂ composites, while the arc erosion was not studied in their research. BRAUMANN and KOFFLER [26] thought that larger oxide particles can achieve equivalent or better

Foundation item: Project (51274163) supported by the National Natural Science Foundation of China; Project (13JS076) supported by the Key Laboratory Research Program of Shaanxi Province, China; Project (2012KCT-25) supported by the Pivot Innovation Team of Shaanxi Electrical Materials and Infiltration Technique, China; Project (2011HBSZS009) supported by the Special Foundation of Key Disciplines, China

Corresponding author: Xian-hui WANG; Tel: +86-29-82312185; E-mail: xhwang693@xaut.edu.cn

DOI: 10.1016/S1003-6326(16)64168-7

switching performance of AgSnO_2 contact materials whereas the reason why AgSnO_2 contact material with larger oxide particles has a good arc erosion behavior is not clarified.

From the aforementioned study, it can get some understanding of the arc erosion mechanism of AgSnO_2 contact material, but the effect of SnO_2 particle size on the arc erosion behavior of AgSnO_2 contact material is still unclear. As the properties depend on the microstructure, the SnO_2 particle size inevitably affects the erosion behavior of AgSnO_2 contact material. Consequently, it is of significance to gain deep insights of the effect of SnO_2 particle size on the arc erosion behavior of AgSnO_2 contact material. In the present work, Ag-4\%SnO_2 (mass fraction) contact materials with different SnO_2 particle sizes were fabricated by powder metallurgy. The effect of SnO_2 particle size on the microstructure and properties of Ag-4\%SnO_2 contact materials was studied, and the mechanism of arc erosion was discussed.

2 Experimental

Ag powder (purity $\geq 99.9\%$, particle size of $73 \mu\text{m}$) and SnO_2 powder (purity $\geq 99.8\%$, particle sizes of 300 and 800 nm) were used to fabricate AgSnO_2 contact materials. The morphologies of the starting Ag powder and SnO_2 powder were characterized by a JSM-6700F scanning electron microscope (Fig. 1), and the particle size distribution of the starting SnO_2 powder was analyzed by a BT-2003 laser diffraction-based particle size analyzer (Fig. 2). The Ag and SnO_2 powders with a mass ratio of 96:4 were mixed for 6 h in a custom-made vibrating mill containing agate balls at a mass ratio of ball to powder of 40:1 and a rotational speed of 200 r/min, and 1% (mass fraction) absolute ethyl alcohol was adopted as process control agent during milling. The relative density of green compact was pre-set as 75% by controlling the compact dimension and mass. The composite powder was compressed in a closed die on a TM-106 hydraulic press under a pressure of 300 MPa for 40 s to obtain a compact with a cylindrical shape, 15 mm in diameter and 7 mm in thickness, followed by sintering at $700 \text{ }^\circ\text{C}$ for 2 h under argon gas. The electrical conductivity and hardness were tested on a 7501 eddy electrical conductivity gauge and a HB-3000 Brinell hardness tester under the load of 2500 N holding for 30 s, respectively, and the values were the average of three measured results. The density was measured utilizing Archimedes method. The microstructure of Ag-4\%SnO_2 contact materials was examined by a GX71 Olympus microscope.

The arc erosion was tested in an arc extinguishing chamber modified by a TDR240A crystal furnace, and

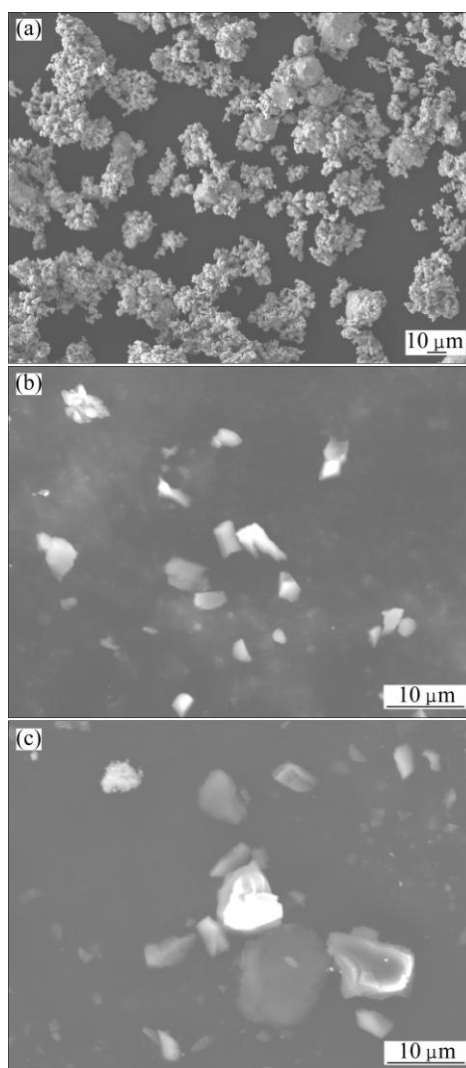


Fig. 1 Morphologies of starting Ag powder (a), 300 nm SnO_2 powder (b) and 800 nm SnO_2 powder (c)

the circuit of vacuum electrical breakdown is shown in Fig. 3. The sample as a cathode was put in a Cu platform, which can move up and down in the vacuum chamber. Above the cathode, there was a pure tungsten rod with a radius of 5 mm and a tip radius of 1 mm as the anode. When the chamber was evacuated to $5.0 \times 10^{-3} \text{ Pa}$ and the capacitor of $120 \mu\text{F}$ was charged at the voltage of 3.5 kV, the cathode moved upward at a velocity of 0.2 mm/min until the gap was broken down, and then the cathode moved back to its initial position, and the gap between cathode and anode was 0.5 mm. The operations were repeated 50 times. The arc duration can be collected from the discharged waveform recorded by a Tektronix TDS-2014 dual channel digital memory oscilloscope. The mass of Ag-4\%SnO_2 contact materials before and after arc erosion was measured by a TG328A photoelectric analytical balance, the surface morphologies and compositions of the eroded Ag-4\%SnO_2 contact materials were characterized by a

JSM-6700F scanning electron microscope (SEM) equipped with an energy disperse spectroscopy (EDS), and the erosion areas were calculated by an Image-Pro Plus 6.0 software.

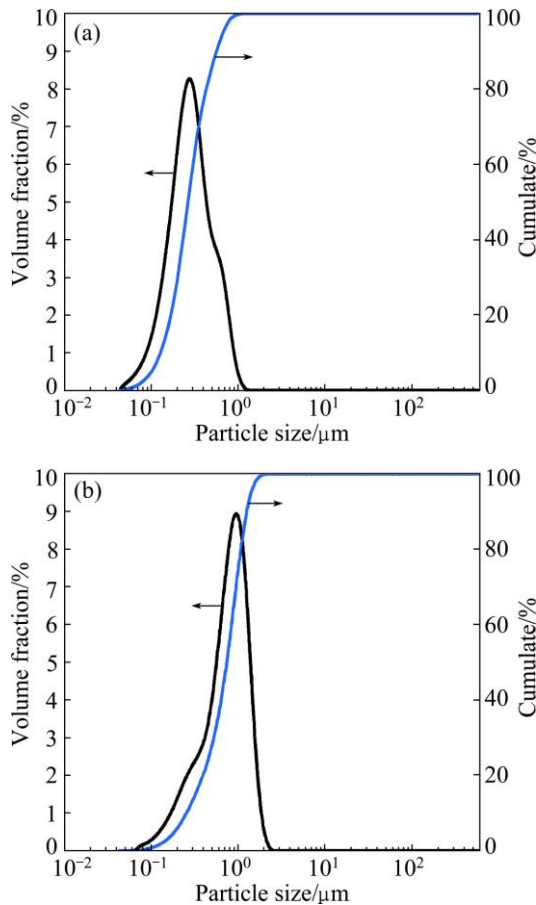


Fig. 2 Particle size distribution of starting 300 nm SnO₂ powder (a) and 800 nm SnO₂ powder (b)

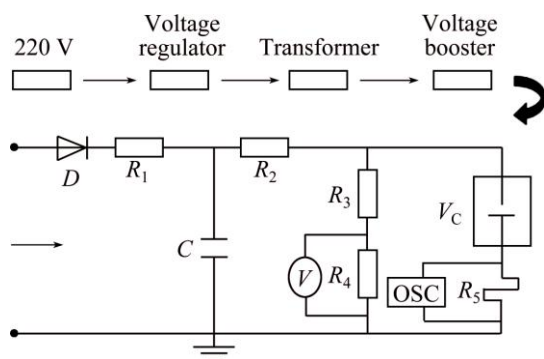


Fig. 3 Circuit of vacuum electrical breakdown

3 Results and discussion

3.1 Effect of SnO₂ particle size on microstructure of Ag-4%SnO₂ contact material

The morphologies and EDS mappings of Ag-SnO₂ mixed powders prepared by 300 nm SnO₂ powder and 800 nm SnO₂ powder are given in Fig. 4. The red regions

in Figs. 4(a₂) and (b₂) represent the distribution of Ag, and the green regions in Figs. 4(a₃) and (b₃) represent the distribution of Sn, while the yellow regions in Figs. 4(a₄) and (b₄) represent the distribution of O. As seen from Fig. 4, the Ag-SnO₂ powders are mixed well after milling for 6 h at a mass ratio of ball to powder of 40:1 and a rotational speed of 200 r/min.

Figures 5(a) and (b) show the microstructures of Ag-4%SnO₂ contact materials prepared by 300 and 800 nm SnO₂ powders, respectively. The dark regions are SnO₂ particles, while the gray regions are Ag matrix. As seen from Fig. 5(a), the distribution of SnO₂ particles is relatively uniform on the Ag matrix for the Ag-4%SnO₂ contact material prepared with 300 nm SnO₂ powder. However, when the SnO₂ particle size is 800 nm, there exists an obvious agglomeration in the Ag-4%SnO₂ contact material, as shown in Fig. 5(b).

3.2 Effect of SnO₂ particle size on properties of Ag-4%SnO₂ contact material

Table 1 lists the relative density, hardness and electrical conductivity of Ag-4%SnO₂ contact materials prepared by 300 and 800 nm SnO₂ powders. With the increase of SnO₂ particle size, the relative density and hardness of Ag-4%SnO₂ contact material decrease, while the electrical conductivity increases. This is because fine SnO₂ particles increase the contact area between the Ag matrix and SnO₂ particles, thus promoting the formation and growth of sintering necks. Moreover, fine SnO₂ particles have larger surface energy, which is beneficial for sintering, giving rise to more densification of Ag-4%SnO₂ contact material. The difference of hardness can be derived from the different strengthening effects of SnO₂ particle sizes. According to the Hall-Petch equation [27], the hardness of AgSnO₂ contact material increases with the decrease of SnO₂ size. Compared with the Ag-4%SnO₂ contact material prepared with 300 nm SnO₂ powder, the electrical conductivity of Ag-4%SnO₂ contact material prepared with 800 nm SnO₂ powder is increased by 62.60%. This can be ascribed to the combined effect of the poor densification and interfaces to electron scattering [28], but the interfaces may play a more significant role, thus giving rise to a higher electrical conductivity for the Ag-4%SnO₂ contact material prepared with 800 nm SnO₂ powder.

3.3 Effect of SnO₂ particle size on arc erosion of Ag-4%SnO₂ contact material

Figures 6(a) and (b) are the change of arc duration with operation times of Ag-4%SnO₂ contact materials prepared with 300 and 800 nm SnO₂ powders, respectively. It can be seen from Fig. 6(a) that the arc duration of Ag-4%SnO₂ contact material prepared

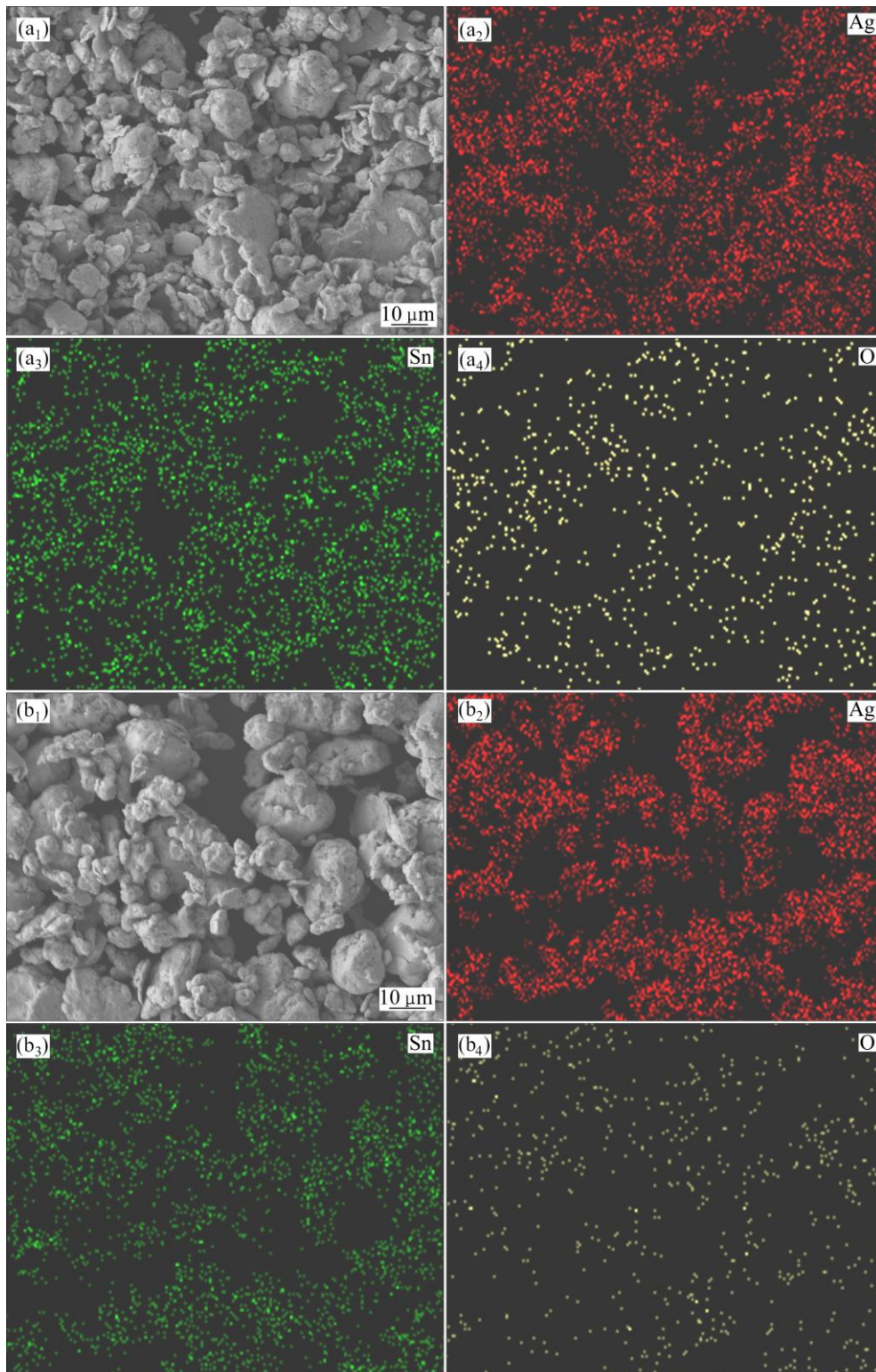


Fig. 4 Morphologies (a_1 , b_1) and EDS mappings (a_2 – a_4 , b_2 – b_4) of Ag–SnO₂ mixed powders prepared with 300 nm SnO₂ powder (a_1 – a_4) and 800 nm SnO₂ powder (b_1 – b_4)

with 300 nm SnO₂ powder has a less fluctuation at the first 20 times and a large fluctuation at the last 30 times, and the average arc duration is 15.9 ms with a standard deviation of 1.93. However, for the Ag–4%SnO₂ contact material prepared with 800 nm SnO₂ powder, there is a

large fluctuation of arc duration during the whole process, and the average arc duration is 19.27 ms with a standard deviation of 2.17, as shown in Fig. 6(b). The reason why the arc duration of Ag–4%SnO₂ contact material prepared with 300 nm SnO₂ powder has a less

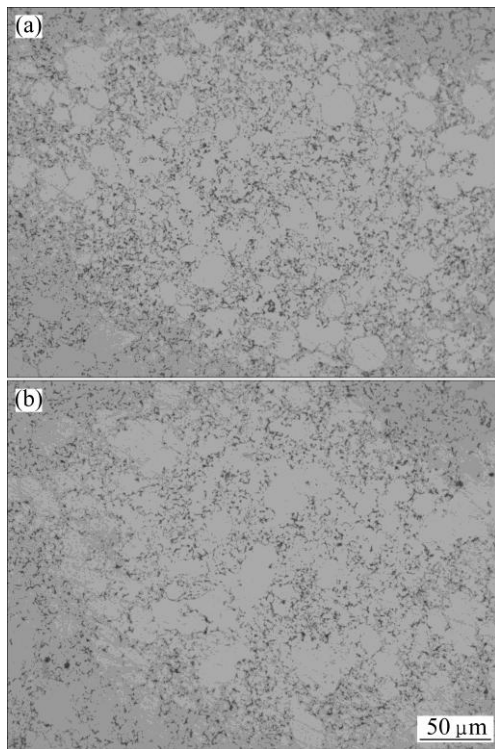


Fig. 5 Microstructures of Ag-4%SnO₂ contact materials prepared by 300 nm SnO₂ powder (a) and 800 nm SnO₂ powder (b)

Table 1 Relative density, hardness and electrical conductivity of Ag-4%SnO₂ contact materials prepared with different SnO₂ particle sizes

SnO ₂ size/nm	Relative density/%	Hardness (HB)	Electrical conductivity/%IACS
300	89.3	31.7	27.0
800	77.7	28.3	43.9

change is that the fine SnO₂ particles distribute uniformly in the Ag matrix. The surface of Ag-4%SnO₂ contact material suffers less deterioration at the early stage of arc erosion, resulting in the approximate arc duration. With the increase of operation times, the accumulated arc energy leads to the formation of uneven surface, causing a larger fluctuation of arc duration. When SnO₂ particles are coarse, the ion bombardment and splash of molten droplets are prone to occur, and the surface of Ag-4%SnO₂ contact material deteriorates seriously, which leads to a large fluctuation of arc duration. This suggests that fine SnO₂ particles are favorable for the improvement on the arc erosion resistance.

As for the better arc erosion resistance of Ag-4%SnO₂ contact material prepared with 300 nm SnO₂ powder, it can be explained as follows. The fine SnO₂ particles cannot offer enough metallic vapors to sustain arc combustion for a long time. Moreover, the

SnO₂ particles in the Ag-4%SnO₂ contact material prepared with 300 nm SnO₂ powder disperse in the Ag matrix more uniformly and the arc erosion becomes relatively dispersive when compared with those in the Ag-4%SnO₂ contact material prepared with 800 nm SnO₂ powder. The combined effect of the two factors gives rise to better arc erosion resistance of Ag-4%SnO₂ contact material prepared with 300 nm SnO₂ powder.

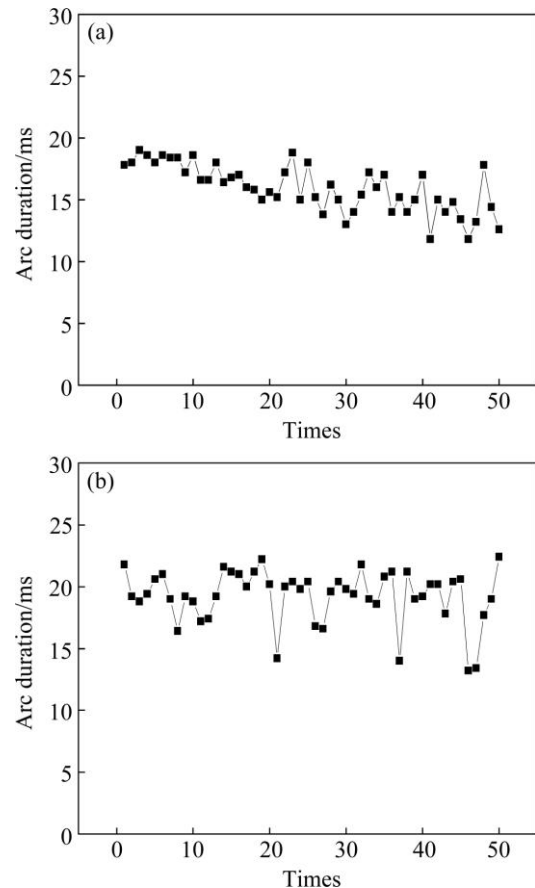


Fig. 6 Change of arc duration with operation times for Ag-4%SnO₂ contact materials prepared with 300 nm SnO₂ powder (a) and 800 nm SnO₂ powder (b)

The mass of Ag-4%SnO₂ contact materials prepared with 300 and 800 nm SnO₂ powders before and after arc erosion 50 times are listed in Table 2. It is obvious that the Ag-4%SnO₂ contact material prepared with 800 nm SnO₂ powder has more mass loss than that prepared with 300 nm SnO₂ powder. This is in good agreement with the arc duration.

Table 2 Mass change of Ag-4%SnO₂ contact materials prepared with different SnO₂ particle sizes before and after arc erosion 50 times

SnO ₂ size/nm	$m_{\text{before}}/\text{g}$	$m_{\text{after}}/\text{g}$	$\Delta m/\text{mg}$	Mass loss rate/%
300	9.0045	9.0034	-1.1	0.012
800	9.5121	9.5101	-2.0	0.021

Figure 7 shows the surface morphologies of Ag–4%SnO₂ contact materials prepared with 300 and 800 nm SnO₂ powders after arc erosion 50 times at different magnifications. It can be seen from Figs. 7(a₁) and (b₁) that the arc erosion occurs on a larger area for the Ag–4%SnO₂ contact material prepared with 300 nm SnO₂ powders than that for the Ag–4%SnO₂ contact material prepared with 800 nm SnO₂ powder, and the erosion areas measured are 4.56 and 3.23 mm², respectively. As seen from Figs. 7(a₂) and (a₃), more dispersed and shallower erosion pits present on the Ag–4%SnO₂ contact material prepared with 300 nm SnO₂ powder. With the increase of SnO₂ particle size, the arc erosion area becomes more concentrated, thus leading to the formation of larger and deeper erosion pits, as shown in Figs. 7(b₂) and (b₃). Additionally, it can also be seen from Fig. 7(b₃) that there are obvious traces of flow and solidification of molten silver, spherical particles and large pits. This suggests that fine SnO₂ particle size is beneficial for the improvement of the arc

erosion resistance of Ag–4%SnO₂ contact material.

Generally, it is believed that arc erosion prefers to occur on the phase with a low electron work function, and the arc motion is closely related to the phase size [29,30]. Since the electron work functions of Ag and SnO₂ are 4.70 and 3.54 eV, respectively, the arc prefers to generate on the SnO₂ particles. For coarse SnO₂ particles, the arc can dwell on a site for a long period until it cannot be sustained, and subsequently hops to the adjacent one. The accumulated thermal energy results in larger and much deep erosion pits. However, the metallic vapor for arc to combustion is relatively less for fine SnO₂ particles. Once SnO₂ is exhausted, the arc moves to another site, resulting in a rapid arc motion. As a result, arc erosion is concentrated on a larger area and the erosion pits become shallower.

The effect of SnO₂ particle size on the characteristics of arc motion can be further verified by the marginal surface morphologies of eroded Ag–4%SnO₂ contact materials prepared with 300 and 800 nm

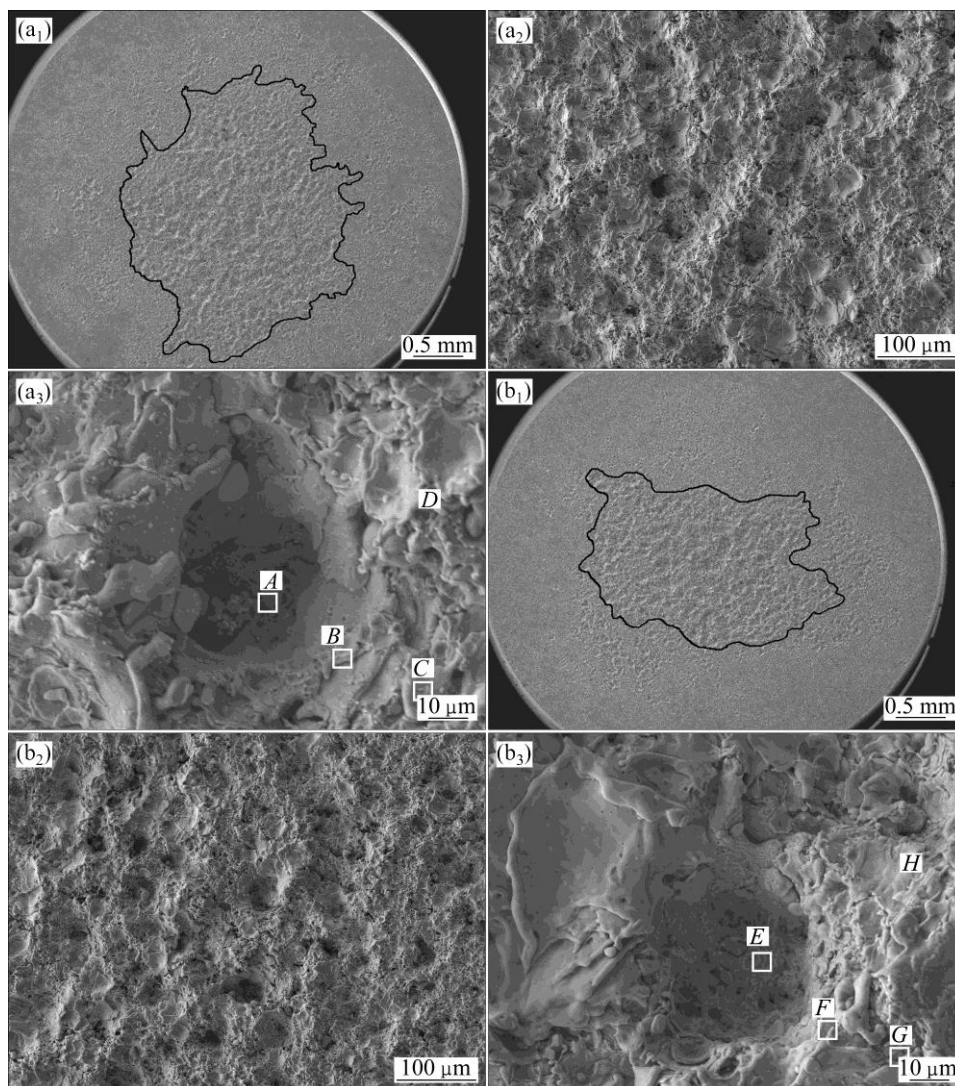


Fig. 7 Surface morphologies of Ag–4%SnO₂ contact materials prepared with 300 nm SnO₂ powder (a₁–a₃) and 800 nm SnO₂ powder (b₁–b₃) after arc erosion 50 times

SnO₂ powders, as shown in Figs. 8(a) and (b). As seen from Fig. 8(a), the Ag–4%SnO₂ contact material prepared with 300 nm SnO₂ powder has more continuous erosion pits, whereas the Ag–4%SnO₂ contact material prepared with 800 nm SnO₂ powder presents discontinuous erosion pits, as shown in Fig. 8(b). This demonstrates that the arc motion changes from random hopping to relatively continuous movement with the decrease of SnO₂ particle size.

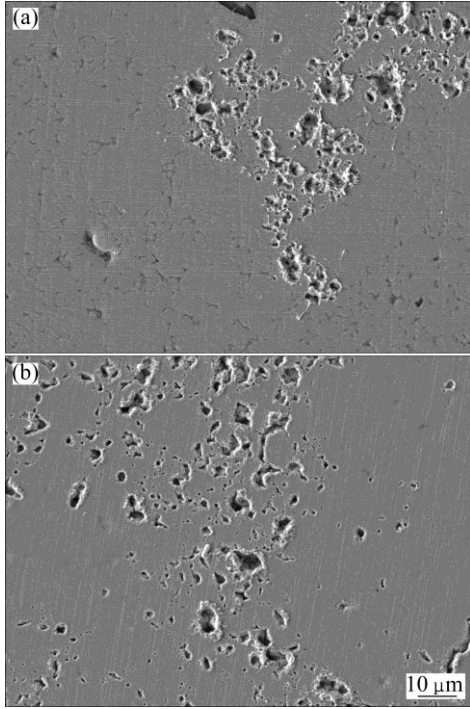


Fig. 8 Marginal surface morphologies of eroded Ag–4%SnO₂ contact materials prepared with 300 nm SnO₂ powder (a) and 800 nm SnO₂ powder (b) after arc erosion 50 times

To determine the surface compositions of eroded Ag–4%SnO₂ contact materials, point analyses by EDS in zones A, B, C, D, E, F, G and H shown in Fig. 7 are listed in Table 3. From the EDS analyses of points A, B, C, E, F and G, it is clear that the surface composition of Ag–4%SnO₂ contact material prepared with 300 nm SnO₂ powder is relatively homogeneous. The EDS results of zones D and H show that the latter has a higher SnO₂ content, which indicates that more pronounced erosion of the Ag–4%SnO₂ contact material prepared with 800 nm SnO₂ powder occurs in comparison with that of the Ag–4%SnO₂ contact material prepared with 300 nm SnO₂ powder. This is derived from the poor wettability between molten Ag and SnO₂ particles. According to the analysis of acting force to the SnO₂ particles (Eq. (1)), the floating acceleration of SnO₂ particles in the molten pool is achieved, as shown in Eq. (2). It is learnt from Eq. (2) that the large SnO₂ particles are more easier to reach the surface, which leads to the decreased viscosity at the bottom of the

molten pool, so the splash of the molten Ag occurs easily. Whereas, fine SnO₂ particles can dwell on the molten pool for a long time, thus inhibiting the sputter erosion under the turbulent of molten pool. Consequently, the Ag–4%SnO₂ contact material prepared with 300 nm SnO₂ powder exhibits better arc erosion resistance.

$$\rho_{\text{Ag}} \left(\frac{4}{3} \pi r^3 \right) g - \left[6\pi \eta r v_{\infty} + \rho_{\text{SnO}_2} \left(\frac{4}{3} \pi r^3 \right) g \right] = \rho_{\text{SnO}_2} \left(\frac{4}{3} \pi r^3 \right) a \quad (1)$$

$$a = \frac{1}{\rho_{\text{SnO}_2}} \left[(\rho_{\text{Ag}} - \rho_{\text{SnO}_2}) g - \frac{9\eta v_{\infty}}{2r^2} \right] \quad (2)$$

where ρ_{SnO_2} and ρ_{Ag} are the densities of SnO₂ and Ag, respectively, r is the radius of SnO₂ particle, η and v_{∞} are the coefficient of dynamic viscosity and kinematic viscosity, respectively, and g is the acceleration of gravity.

Table 3 EDS results of zones A, B, C, D, E, F, G and H shown in Fig. 7

Element	Mass fraction/%							
	A	B	C	D	E	F	G	H
Ag	96.41	94.16	98.94	96.58	95.00	93.49	99.08	94.05
Sn	3.59	5.84	1.06	3.42	5.00	6.51	0.92	5.95

4 Conclusions

1) Fine SnO₂ particles increase the relative density and hardness of Ag–4%SnO₂ contact material, while decrease the electrical conductivity.

2) The Ag–4%SnO₂ contact material prepared with 300 nm SnO₂ powder has shorter arc duration and less mass loss in comparison with the Ag–4%SnO₂ contact material prepared with 800 nm SnO₂ powder.

3) Fine SnO₂ particles enhance the arc erosion resistance of Ag–4%SnO₂ contact material. The Ag–4%SnO₂ contact material prepared with 300 nm SnO₂ powders presents larger erosion area and shallower and more dispersed arc erosion pits.

References

- [1] WANG X H, YANG H, CHEN M, ZOU J T, LIANG S H. Fabrication and arc erosion behaviors of AgTiB₂ contact materials [J]. Powder Technology, 2014, 256: 20–24.
- [2] TAO Qi-ying, ZHOU Xiao-long, ZHOU Yun-hong, ZHANG Hao. Electrical contact properties of AgCuO electrical contact materials [J]. The Chinese Journal of Nonferrous Metals, 2015, 25(5): 1244–1249. (in Chinese)
- [3] COSOVIC V, COSOVIC A, TALIJAN N, ZIVKOVIC D, MANASIJEVIC D, MINIC D. Improving dispersion of SnO₂ nanoparticles in Ag–SnO₂ electrical contact materials using template method [J]. Journal of Alloys and Compounds, 2013, 567: 33–39.
- [4] WU C P, YI D Q, LI J, XIAO L R, WANG B, ZHENG F. Investigation on microstructure and performance of Ag/ZnO contact material [J]. Journal of Alloys and Compounds, 2008, 457: 565–570.

- [5] YE Jia-jian, XIONG Wei-hao, XU Jian, FU Jiang-hua, LI Zhen-biao. Research progress in AgSnO₂ contact material in low-voltage relay [J]. Materials Review, 2007, 21(2): 87–90. (in Chinese)
- [6] BIYIK S, ARSLAN F, AYDIN M. Arc-erosion behavior of boric oxide-reinforced silver-based electrical contact materials produced by mechanical alloying [J]. Journal of Electronic Materials, 2015, 44(1): 457–466.
- [7] WANG J, LI D M, WANG Y P. Microstructure and properties of Ag–SnO₂ materials with high SnO₂ content [J]. Journal of Alloys and Compounds, 2014, 582: 1–5.
- [8] COSOVIC V, PAVLOVIC M, COSOVIC A, VULIC P, PREMOVIC M, ZIVKOVIC D, TALJAN N. Microstructure refinement and physical properties of Ag–SnO₂ based contact materials prepared by high-energy ball milling [J]. Science of Sintering, 2013, 45(2): 173–180.
- [9] ZHOU Zhao-feng, GAN Wei-ping. Development of AgSnO₂ contact material [J]. Rare Metals and Cemented Carbides, 2004, 32(2): 53–56. (in Chinese)
- [10] LIN Z J, LIU S H, SUN X D, XIE M, LI J G, LI X D, CHEN Y T, CHEN J L, HUO D, ZHANG M, ZHU Q, LIU M M. The effects of citric acid on the synthesis and performance of silver–tin oxide electrical contact materials [J]. Journal of Alloys and Compounds, 2014, 588: 30–35.
- [11] XU Can-hui, YI Dan-qing, CAO Shi-yi, LIU Hui-qun, WU Chun-ping, SUN Shun-ping, LIU Run-yong. Hot compression behavior of AgSnO₂ composite material [J]. The Chinese Journal of Nonferrous Metals, 2011, 21(9): 2091–2098. (in Chinese)
- [12] YANG Tian-zu, DU Zuo-juan, GU Ying-ying, QIU Xiao-yong, JIANG Ming-xi, CHU Guang. Preparation of flake AgSnO₂ composite powders by hydrothermal method [J]. Transactions of Nonferrous Metals Society of China, 2007, 17(2): 434–438.
- [13] RIEDER W, WEICHSLER V. Make erosion mechanism of AgCdO and AgSnO₂ contact [J]. IEEE Transactions on Components, Hybrids, and Manufacturing Technology, 1992, 15(3): 332–338.
- [14] RONG Ming-zhe. Theory of electrical contact [M]. 1st ed. Beijing: China Machine Press, 2004: 27–29. (in Chinese)
- [15] BEHRENS V, HONIG T, KRAUS A, MICHAL R, SAEGER K, SCHMIDBERGER R, STANEFF T. An advanced silver/tin oxide contact material [C]//Proceeding of the 39th IEEE Holm Conference on Electrical Contacts. Pittsburgh: IEEE, 1993: 19–25.
- [16] DU Yong-guo, YANG Guang, ZHANG Jia-chun, WANG Guang-hua, LONG Yan. Physical metallurgy analysis of arc erosion of AgMeO contact material [J]. Electrical Engineering Materials, 1997, 4: 1–8. (in Chinese)
- [17] ZHU Yan-cai, WANG Jing-qin, WANG Hai-tao. Study on arc erosion resistance properties of nano-AgSnO₂ electrical contact materials doped with Bi [J]. Rare Metal Material and Engineering, 2013, 42(1): 149–152. (in Chinese)
- [18] ZHU Y C, WANG J Q, WANG H T, DING J. Preparation and study on nano-Ag/SnO₂ electrical contact material doped rare earth element [J]. Materials Science Forum, 2014, 789: 270–274.
- [19] LUNGU M, GAVRILIU S, CANTA T, LUCACI M, ENESCU E. AgSnO₂ sintered electrical contacts with ultrafine and uniformly dispersed microstructure [J]. Journal of Optoelectronics and Advanced Materials, 2006, 8(2): 576–581.
- [20] WANG Jun-bo, LI Ying-min, WANG Ya-ping, DING Bing-jun. Study of nanocomposite silver-based contact materials [J]. Rare Metal Material and Engineering, 2004, 33(11): 1213–1217. (in Chinese)
- [21] WITTER G, CHEN Z. A comparison of silver tin indium oxide contact materials using a new model switch that simulates operation of an automotive relay [C]//Proceeding of the 50th IEEE Holm Conference on Electrical Contact and the 22nd International Conference on Electrical Contacts. Seattle: IEEE, 2004: 382–387.
- [22] SWINGLER J, SUMPTION A. Arc erosion of AgSnO₂ electrical contacts at different stages of a break operation [J]. Rare Metals, 2010, 29(3): 248–254.
- [23] XU Jian, XIONG Wei-hao, FU Jiang-hua, LI Zhen-biao. Simulation analysis of effect of second metal-oxide phase on molten pool in Ag-based electrical contact [J]. The Chinese Journal of Nonferrous Metals, 2008, 18(7): 1323–1329. (in Chinese)
- [24] ZHANG Kun-hua, GUAN Wei-ming, SUN Jia-lin, LU Feng, CHEN Jing-chao, ZHOU Xiao-long, DU Yan. Preparation and DC arc erosion morphology of AgSnO₂ contact materials [J]. Rare Metal Material and Engineering, 2005, 34(6): 924–927. (in Chinese)
- [25] LIN Z J, SUN X D, LIU S H, CHEN J L, XIE M, LI J G, LI X D, HUO D, ZHANG M, ZHU Q. Effect of SnO₂ particle size on properties of Ag–SnO₂ electrical contact materials prepared by the reductive precipitation method [J]. Advanced Materials Research, 2014, 936: 459–463.
- [26] BRAUMANN P, KOFFLER A. The influence of manufacturing process, metal oxide content, and additives on the switching behavior of Ag/SnO₂ in relays [C]//Proceeding of the 50th IEEE Holm Conference on Electrical Contact and the 22nd International Conference on Electrical Contacts. Seattle: IEEE, 2004: 90–97.
- [27] HANSEN N. Hall–Petch relation and boundary strengthening [J]. Scripta Materialia, 2004, 51(8): 801–806.
- [28] DU Yong-guo, BAI Shu-xin, YI Yang, ZHANG Jia-chuan. The resistance of tin-oxide particulate-reinforced silver composite materials [J]. Journal of Functional Materials, 1994, 25(2): 150–153. (in Chinese)
- [29] WANG Ya-ping, ZHANG Li-na, DING Bing-jun, ZHOU Jing-en. Effect of selective strengthening of CuCr contact materials on the dielectric strength in a short vacuum gap [J]. Proceedings of the Chinese Society for Electrical Engineering, 1999, 19(3): 47–50. (in Chinese)
- [30] WANG Ya-ping, ZHANG Hui, DING Bing-jun, SUN Jun. Influence of the microstructure of electrode materials on the motion behaviors of vacuum arc cathode spot [J]. Acta Metallurgica Sinica, 2004, 40(12): 1269–1273. (in Chinese)

不同 SnO₂ 粒度制备的 AgSnO₂ 触头材料电弧侵蚀行为

张 苗, 王献辉, 杨晓红, 邹军涛, 梁淑华

西安理工大学 陕西省电工材料与熔(浸)渗技术重点实验室, 西安 710048

摘 要: 为了阐明 SnO₂ 粒度大小对 AgSnO₂ 触头材料电弧侵蚀行为的影响, 采用粉末冶金法制备不同 SnO₂ 粒度的 Ag–4%SnO₂(质量分数)触头材料, 对触头材料组织进行观察, 并对其致密度、硬度和导电率进行测量。对 Ag–4%SnO₂ 触头材料进行电弧侵蚀实验, 确定燃弧时间和电弧侵蚀前后的质量变化, 并对电弧侵蚀后触头材料表面的形貌和成分进行表征。结果表明: 细小的 SnO₂ 颗粒有助于提高 Ag–4%SnO₂ 触头材料的致密度和硬度, 但降低了其导电率。随着 SnO₂ 粒度的减小, Ag–4%AgSnO₂ 触头材料的燃弧时间变短, 质量损失降低, 电弧侵蚀面积增大, 蚀坑变浅且分散。

关键词: AgSnO₂ 触头材料; SnO₂ 粒度; 电弧侵蚀; 导电率; 硬度

(Edited by Mu-lan QIN)